fire

MDPI

Article

A Refined Theoretical Model for Predicting Jet Fire Length from High-Pressure Hydrogen Leaks: Integration of Real-Gas Effects and Parametric Analysis

Jia-Wen Liu [1,†], Xue-Li Li [1,†], Run-Qi Song [1], Yi Fang [1], En-Ming Zhu [1], Yi-Ming Dai [2], Jeong-Tae Kwon [3], Ji-Qiang Li [1,*] and Yao Wang [4,*]

[1] School of Transportation, Ludong University, Yantai 264025, China
[2] Department of Electronic, Electrical and Systems Engineering, University of Birmingham, Birmingham B15 2TT, UK
[3] Department of Mechanical Engineering, Hoseo University, Asan 31499, Republic of Korea
[4] State Key Laboratory of High-End Compressor and System Technology, Beijing University of Chemical Technology, Beijing 100029, China
* Correspondence: ljq7436@ldu.edu.cn (J.-Q.L.); wy@mail.buct.edu.cn (Y.W.)
† These authors contributed equally to this work.

Abstract

Aiming at the insufficient integration of real-gas effects and the unclear parameter influence mechanisms in predicting high-pressure hydrogen leakage flame length, this paper proposes a refined predictive model that systematically incorporates the real-gas critical flow factor (C_r^*). By dynamically correcting the mass flow rate calculation under high-pressure conditions, the model significantly improves prediction accuracy (relative error in mass flow rate < 3%). A parametric analysis reveals that the flame length is approximately three times more sensitive to the leakage orifice diameter than to the storage pressure ($L \propto D^{1.041} P_0^{0.347}$), providing a quantitative basis for inherent safety design. Validated by experimental datasets, the model demonstrates good accuracy. It can be employed for safety distance demarcation and risk assessment at hydrogen refueling stations and storage facilities.

Keywords: high-pressure hydrogen leakage; jet fire length; real-gas effect; critical flow factor; parametric sensitivity analysis; hydrogen safety

1. Introduction

Jet fires resulting from high-pressure hydrogen leakage constitute a critical risk source in the safety design of hydrogen energy facilities, such as hydrogen refueling stations and onboard storage systems. The accurate prediction of their flame length directly determines the reliability of safety distance demarcation. With a high mass energy density of up to 120 MJ/kg, hydrogen serves as a potent alternative to fossil fuels. Its large-scale application is projected to reduce global carbon dioxide emissions by up to 830 million tons annually, positioning it as one of the most promising energy carriers in global decarbonization efforts [1,2]. As storage pressures advance to 70 MPa and beyond, the real-gas effects of hydrogen during leakage become increasingly pronounced, leading to significant deviations in mass flow calculations when using classical predictive models based on ideal-gas assumptions. Particularly with the rapid growth of the global fuel cell vehicle fleet (Figure 1), high-pressure leakage scenarios are becoming more frequent, underscoring the urgent need for developing accurate flame prediction models.

Check for updates

Academic Editor: Huaming Dai

Received: 21 January 2026
Revised: 8 February 2026
Accepted: 11 February 2026
Published: 24 February 2026

Copyright: © 2026 by the authors. Licensee MDPI, Basel, Switzerland. This article is an open access article distributed under the terms and conditions of the Creative Commons Attribution (CC BY) license.

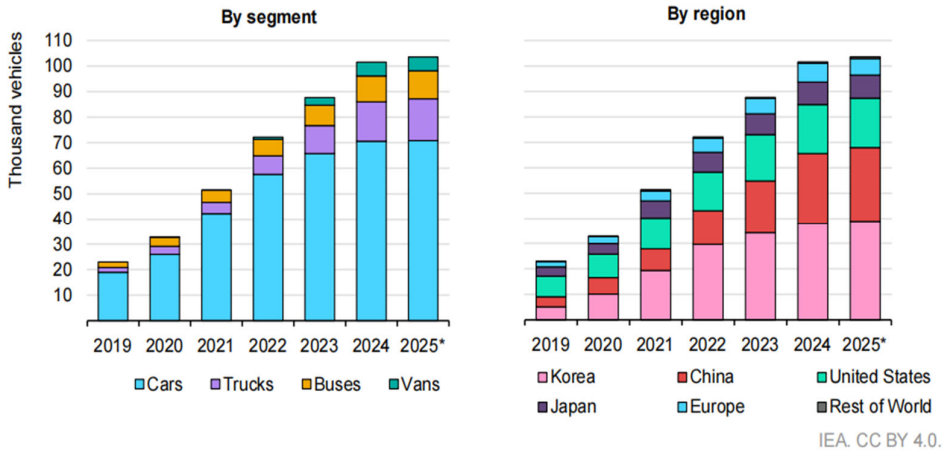


Figure 1. Fuel Cell Electric Vehicle Stock by Segment and Region, 2019–2025. Note: 2025* includes data from January to July.

As shown in Figure 1, the figure illustrates the changing trends in the stock of fuel cell electric vehicles globally and across different regions from 2019 to 2025. Based on data from the International Energy Agency (IEA) Hydrogen Infrastructure Projects database (September 2025), the chart clearly reveals a significant growth in the global deployment and adoption of fuel cell vehicles. With the increasing prevalence of fuel cell vehicle usage, safety concerns related to the vehicles and their surrounding environments are drawing greater attention [3]. Specifically, the rapid increase in the vehicle fleet directly raises the probability of high-pressure hydrogen storage system leaks occurring both in static states (e.g., while parked in lots or service centers) and during operation. Consequently, the accurate prediction of jet flame length—the most hazardous consequence of high-pressure hydrogen leakage—has become a critical research topic for ensuring the safe and sustainable development of the industry, holding vital practical significance.

A substantial body of research has been devoted to the safety of high-pressure hydrogen leakage, with multi-level investigations spanning from leakage and dispersion, auto-ignition mechanisms, and flame characteristics to consequence assessment. Yang et al. [4] systematically reviewed the progress in research on high-pressure hydrogen leakage and dispersion, highlighting the influence of factors such as the geometry of the leakage scenario and the initial pressure. Zou et al. [5], focusing on the leakage process itself, developed a model for the high-pressure gas leakage process that incorporates heat exchange, noting that predictions based on ideal gas models under the isentropic process assumption exhibit significant errors.

Regarding the risk of spontaneous ignition, Cui et al. [6] and Liu et al. [7] conducted in-depth investigations into the shock wave growth patterns and auto-ignition characteristics influenced by factors such as pipeline geometry, obstacles, and pipeline failure. Lin et al. [8] further performed numerical studies on the impact of rupture disk shape and opening characteristics on spontaneous ignition behavior. Zhou et al. [9] employed three-dimensional large eddy simulations to study the spontaneous ignition of high-pressure hydrogen-enriched methane in rectangular ducts, revealing that reflected shock waves and Mach reflections generating hot spots are key mechanisms for triggering auto-ignition. Pan et al. [10] and Huang et al. [11] experimentally and numerically studied, respectively, the suppression effects and flow dynamics of high-pressure hydrogen auto-ignition in relation to leakage orifice area, pipe length, and pipeline configurations (L-shaped, T-shaped). The experimental research by Ayi et al. [12] further indicated that hydrogen auto-ignition is not purely an intrinsic property but is significantly influenced by external risk factors. Cui

et al. [13] investigated the characteristics of in-tube flame propagation and external jet flame evolution following spontaneous ignition during high-pressure hydrogen leakage.

For ignited flames, their morphology and scale are central to consequence assessment. Bradley et al. [14] conducted extensive correlative studies on flame height, lift-off distance, and other parameters of jet flames for various fuels, including hydrogen. Al-Tayyar et al. [15] reviewed measurement techniques and influencing factors for flame height and structure. Lv et al. [16] and Ab Aziz et al. [17] performed experimental measurements and predictions on the geometric characteristics of inclined jet flames and horizontal buoyant jet flames, respectively. Wang et al. [18] further developed a mathematical method for predicting the trajectory length of inclined buoyant jet flames under crosswind conditions. Shen et al. [19] investigated the effects of nozzle shape on the near-field jet structure and far-field concentration distribution. Cerbarano et al. [20], through numerical studies of methane-hydrogen blend fuel leaks in gas turbine enclosures, found that the penetration distance of the axisymmetric flammable cloud for pure hydrogen increased threefold compared to pure methane. Furthermore, while focusing on different fuels and environments, Gain et al. [21] studied RP-3 aviation kerosene and Gao et al. [22] examined diffusion flames under varying gravity levels; their exploration of flame structure and morphology remains valuable for reference.

In the context of high-pressure leakage consequence analysis, Sun et al. [23] developed a consequence analysis method for compressed hydrogen releases, highlighting that the leak orifice size has the most significant impact on explosion overpressure. Liu et al. [24] conducted a consequence analysis for liquid hydrogen storage tank leaks at refueling stations, revealing the dispersion patterns of flammable gas clouds. Meanwhile, Zhang et al. [25] focused on hydrogen refueling stations, and Wang et al. [26] investigated hydrogen leakage, dispersion, and explosion inside fuel cell bus compartments, underscoring the unique risks associated with specific scenarios. Li et al. [27] examined the response behavior and consequences of high-pressure hydrogen storage cylinders under fire conditions. Particularly noteworthy is the work by Weng et al. [28], who, based on a one-dimensional diffusive layer ignition model, studied the influence of real-gas effects on auto-ignition limits under high-pressure conditions, concluding that real-gas effects lead to a higher critical auto-ignition pressure in confined releases. Although differing in scale, the study by Nabizadeh et al. [29] on choked compressible flow in porous media offers insightful methodologies for understanding complex flow phenomena.

While the aforementioned research has enhanced our understanding of the entire chain of high-pressure hydrogen leakage—from dispersion and auto-ignition to combustion and consequences—two clear and critical gaps remain in existing studies concerning the core engineering safety objective of "accurate prediction of jet flame length."

(1). Idealized Deviation in Source Term Calculation and Insufficient Integration of Real-Gas Effects: Most flame length prediction models or correlative studies [14–18] commonly rely on the ideal gas assumption when calculating the leakage source term (mass flow rate). The research by Zou et al. [5] has explicitly indicated errors in models based on the isentropic process. While prior studies have acknowledged real-gas effects in high-pressure hydrogen leakage, none have successfully integrated a dynamically varying C_r^* into a unified flame length prediction model that spans from source term to flame terminal. This study bridges this gap by proposing a holistic model that systematically corrects mass flow rate and flame length predictions under high-pressure conditions.

(2). Unclear Quantitative Influence and Relative Importance of Key Design/Accident Parameters on Flame Length: Regarding the two most critical engineering parameters—storage pressure (P_0) and leakage orifice diameter (D)—there is a lack of systematic

decoupling and quantitative analysis of their individual impacts on flame length and their coupled effects. Although the consequence analysis by Sun et al. [23] indicates that leak orifice size significantly influences explosion outcomes, this qualitative understanding lacks support from quantitative scaling relationships based on the specific hazard form of "flame length." The ambiguity surrounding the sensitivity to these key parameters, particularly the relative importance of P_0 and D, results in a deficiency of precise, quantified theoretical basis for determining safety distances and conducting inherent safety design.

In summary, this study aims to precisely address the aforementioned research gaps by developing a refined predictive model for hydrogen jet flame length applicable to high-pressure conditions. The core innovation lies in achieving a dual correction from source to terminal outcome, which comprises the following specific objectives: (1) To develop a refined predictive model for high-pressure hydrogen jet flame length, overcoming the applicability limitations of traditional models under high-pressure conditions. (2) To introduce a dynamically varying C_r^*, dependent on pressure and temperature, to correct the calculation of the high-pressure leakage source term (mass flow rate), thereby enhancing the model's theoretical accuracy at its origin. (3) To establish a theoretical framework capable of decoupling the effects of pressure and nozzle diameter, systematically revealing their independent influence mechanisms and quantitative scaling relationship on flame length, and clarifying their relative importance, providing a direct and reliable theoretical tool for the safety design and risk assessment of high-pressure hydrogen energy facilities. This research strives not only to enhance the model's predictive accuracy under high pressure but also places particular emphasis on delivering a direct and reliable theoretical tool for the safety design and risk assessment of hydrogen energy installations.

2. Theoretical Model for High-Pressure Hydrogen Leakage Flame Length

2.1. Basic Flame Length Model

The prediction of jet fire flame length is fundamental to fire safety engineering. For stable turbulent diffusion flames, their length is closely related to the fuel release rate. Based on fits to extensive experimental data, previous research has established empirical formulas for predicting hydrogen jet flame length. These formulas directly correlate flame length with fuel mass flow rate and leakage orifice diameter, offering the advantages of concise form and clear physical significance.

This paper employs a well-established empirical correlation widely cited in the field of hydrogen safety to predict the flame length [30], which is presented as follows:

$$L_1 = 76 \cdot (m \cdot D)^{\mathrm{n}} \tag{1}$$

$$L_m = 116 \cdot (m \cdot D)^{\mathrm{n}} \tag{2}$$

In the equation, L_l represents the optimal-fit flame length (in meters); L_m denotes the maximum safety flame length (in meters), which is intended to provide a conservative estimate for safety distance demarcation. m is the mass flow rate of hydrogen (in kg/s); D is the diameter of the circular leakage orifice (in meters); and the exponent n has an empirical value of 0.347.

Figure 2 schematically compares the typical ranges of two flame length definitions—L_l and L_m—for a high-pressure hydrogen leak, clarifying their distinct engineering significance. L_l represents the time-averaged visible flame length, whereas L_m denotes the maximum instantaneous extension due to turbulent pulsations and unsteady combustion. This distinction is critical, as the use of L_m embodies a "conservative" principle in safety design, ensuring protections account for worst-case flame reach.

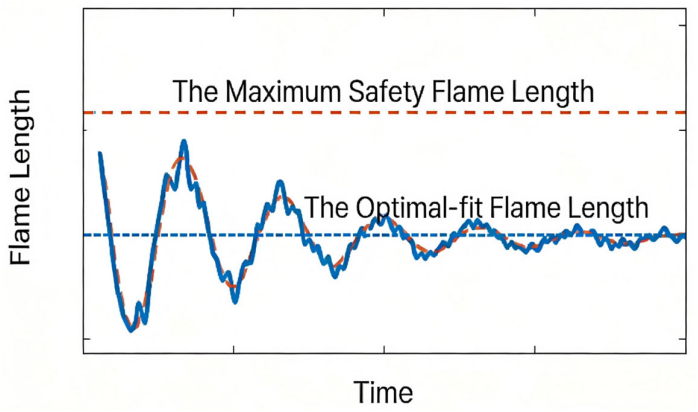


Figure 2. Comparison of the Definitions of Flame Length: The Optimal-fit Flame Length and The Maximum Safety Flame Length.

2.2. Modeling of Mass Flow Rate in High-Pressure Hydrogen Compressible Jets

During a leak from a high-pressure hydrogen storage system, such as a 70 MPa onboard storage tank, the flow at the leakage orifice is typically compressible flow. When specific conditions are met, a choked flow condition can occur. In this case, the calculation of the mass flow rate must be based on the theory of compressible fluid dynamics.

2.2.1. Choked Flow Criteria and Ideal-Gas Mass Flow Rate Formula

Choked flow occurs at the leakage orifice when the ratio of the downstream ambient pressure, P_b, to the upstream storage pressure, P_0, falls below a critical value, at which point the flow velocity reaches the speed of sound. For an ideal gas, this critical pressure ratio is determined by the adiabatic index, γ:

$$\frac{\mathrm{P_b}}{P_0} \leq \left(\frac{2}{\gamma+1}\right)^{\frac{\gamma}{\gamma-1}} \tag{3}$$

For hydrogen, the adiabatic index γ is approximately 1.41. Substituting this value into the equation above yields a critical pressure ratio of approximately 0.528. Therefore, choked flow occurs when $\frac{\mathrm{P_b}}{P_0} \leq 0.528$. Under this condition, the ideal-gas mass flow rate, $q_{m,ideal}$, can be expressed as:

$$q_{m,ideal} = \frac{C_d \cdot A_t \cdot P_0 \cdot \mathrm{C_i^*}}{\sqrt{\mathrm{R_m} \cdot T_0}} \tag{4}$$

In the equation, C_d is the discharge coefficient. In this model, a value of $C_d = 0.75$ is adopted, based on the following rationale: the study by Bobovnik et al. [31] indicates that the discharge coefficient for hydrogen is highly consistent with those for air and nitrogen. For scenarios involving high-pressure hydrogen leakage through non-standard, sharp-edged orifices (such as those resulting from pressure vessel ruptures or valve failures), and with reference to fluid mechanics principles and common practices in safety engineering, the typical value of C_d generally falls within the range of 0.6 to 0.8. Therefore, the value $C_d = 0.75$ used in this study represents a reasonable choice that aligns with the latest experimental findings and adheres to the principle of conservatism in engineering. A_t is the leakage orifice area; R_m is the specific gas constant for hydrogen, 4124 J/(kg·K); and T_0 is the hydrogen storage temperature (K).

Where:

$$A_t = \frac{\pi D^2}{4} \tag{5}$$

C_i^* represents the ideal-gas critical flow factor. For an ideal gas, this factor remains constant and is defined by the following expression:

$$C_i^* = \sqrt{\gamma\left(\frac{2}{\gamma+1}\right)^{\frac{\gamma+1}{\gamma-1}}} \quad (6)$$

For hydrogen, $C_i^* \approx 0.687$.

2.2.2. Integration of the Real-Gas Critical Flow Factor C_r^*

The aforementioned ideal-gas model provides a reasonable approximation at lower pressures. However, under high-pressure conditions, the intermolecular forces and finite molecular volume of hydrogen become non-negligible, causing its behavior to deviate significantly from the ideal-gas assumption. Persisting with the constant C_i^* under these conditions would introduce substantial errors in the calculated mass flow rate, consequently compromising the accuracy of subsequent flame length predictions.

To accurately describe the behavior of high-pressure hydrogen, drawing on the work of Ding et al. [32], it is essential to introduce the C_r^*. Unlike its ideal-gas counterpart, C_r^* is not a constant but rather a function of temperature T_0 and P_0. Its value is determined through precise calculations based on a validated real-gas equation of state. In this study, utilizing established real-gas property data, the variation of C_r^* with T_0 and P_0 is presented in Table 1.

Table 1. Values of the real-gas critical flow factor C_r^* at various temperatures and pressures [32].

The Real-Gas Critical Flow Factors, C_r^*, for Normal Hydrogen											
T (K)	**p (MPa)**										
	0.01	0.05	0.1	1	2	5	10	20	40	70	100
150	0.703504	0.703529	0.70356	0.704088	0.704615	0.705715	0.705675	0.699161	0.67252	0.627066	0.587296
180	0.697025	0.69702	0.697014	0.696889	0.696717	0.695948	0.693728	0.686088	0.663659	0.626718	0.593268
210	0.692632	0.692614	0.692591	0.69217	0.691683	0.690085	0.686921	0.678878	0.658852	0.62714	0.598039
240	0.689706	0.689681	0.689651	0.689092	0.688461	0.686492	0.682933	0.674863	0.656513	0.628343	0.60237
270	0.687763	0.687735	0.687701	0.687082	0.686389	0.684268	0.680579	0.672667	0.655628	0.630061	0.606451
300	0.68648	0.686452	0.686416	0.685776	0.685063	0.6829	0.679213	0.67155	0.655603	0.632065	0.610318
330	0.685643	0.685615	0.685579	0.68494	0.684227	0.682081	0.678464	0.671088	0.656083	0.634199	0.613972
360	0.685107	0.685079	0.685044	0.684415	0.683716	0.681617	0.673105	0.671028	0.656854	0.636359	0.617409
390	0.68477	0.684743	0.684709	0.684097	0.683418	0.681381	0.677989	0.67121	0.657779	0.638481	0.620627
420	0.684563	0.684536	0.684503	0.683911	0.683254	0.681287	0.678022	0.671533	0.658772	0.640522	0.623625
450	0.684435	0.684409	0.684377	0.683806	0.683173	0.681279	0.678141	0.673928	0.659778	0.642459	0.626411
480	0.684353	0.684329	0.684298	0.683748	0.683138	0.681317	0.678304	0.672354	0.660763	0.644279	0.628991
510	0.684295	0.684271	0.684242	0.683713	0.683127	0.681376	0.678483	0.672781	0.661706	0.645979	0.631378
540	0.684246	0.684223	0.684195	0.683686	0.683123	0.681441	0.678663	0.673194	0.662594	0.647558	0.633583
570	0.684195	0.684174	0.684146	0.683658	0.683116	0.681499	0.678831	0.673583	0.663423	0.64902	0.63561
600	0.684138	0.684117	0.684091	0.683621	0.6831	0.681546	0.678981	0.67394	0.66419	0.650371	0.637499

Analysis of the table above reveals that, at a constant temperature, C_r^* decreases significantly with increasing pressure. Conversely, at a constant pressure, C_r^* exhibits a comparatively minor variation with temperature. The substitution of C_i^* with C_r^* constitutes a central step in enhancing the accuracy of mass flow rate calculations for high-pressure hydrogen leaks and represents one of the key innovations of the proposed model.

2.2.3. Real-Gas Mass Flow Rate Equation

The final high-pressure hydrogen leakage mass flow rate calculation model is derived by substituting the C_r^* into the mass flow rate equation:

$$q_{m,real} = \frac{C_d \cdot A_t \cdot P_0 \cdot C_r^*}{\sqrt{R_m \cdot T_0}} \quad (7)$$

This formula comprehensively accounts for the leakage geometric parameters (C_d, A_t), the initial state parameters (P_0, T_0), and the real-gas properties of high-pressure hydrogen (C_r^*).

2.3. Comprehensive Flame Length Model

The final integrated flame length prediction model is formulated by introducing the precise mass flow rate model $\dot{q}_{m,real}$ (Section 2.2) into the foundational model for flame length (Section 2.1).

By substituting Equations (5) and (7) into Equations (1) and (2) and simplifying, we obtain:

$$L = K \cdot \left[\frac{C_d \cdot \pi \cdot D^3 \cdot P_0 \cdot C_r^*}{4\sqrt{R_m \cdot T_0}} \right]^{0.347} \quad (8)$$

where the optimal-fit flame length L_l is calculated with $K = 76$, and the maximum safety flame length L_m is defined for $K = 116$.

The model reveals that flame length scales as $L \propto D^{1.041} P_0^{0.347}$, indicating a stronger dependence on orifice diameter than on storage pressure. This quantitative relationship highlights that the influence of the D on the flame length is more pronounced than that of the storage pressure P_0.

2.4. Model Assumptions and Applicability Range

The development and application of this model are based on a set of explicit assumptions. The core assumptions are as follows: the leakage flow is in a choked flow regime (satisfying $P_b / P_0 \leq 0.528$); the leaking medium is pure hydrogen, and the process is treated as isothermal leakage, neglecting temperature changes due to the Joule-Thomson effect; the leakage orifice is a sharp-edged circular orifice; and the environment is a quiescent; the environment is a calm and still atmosphere without wind, and the flame burns in standard dry air (with an oxygen volume fraction of approximately 20.95%).These conditions collectively define the idealized application scenario of the model, enabling it to clearly reveal the dominant influence patterns of key parameters such as pressure and orifice diameter on flame length. Consequently, this also implies that the model has limitations when dealing with complex real-world scenarios such as non-choked flow, strong wind interference, or significant throttling cooling effects. Addressing these complexities represents a direction for future research to deepen and refine the model.

2.5. Model Validation

To ensure the accuracy and reliability of the proposed refined theoretical model, this section employs two sets of representative independent public experimental data for its systematic validation. The validation strategy is designed to assess the model's performance under two distinct leakage scenarios: (1) to verify the model's predictive capability under typical ultra-high-pressure (>70 MPa) choked release conditions representative of onboard hydrogen storage systems, and (2) to examine its applicability within the medium-to-high pressure range (4–9 MPa) common in facilities such as hydrogen refueling stations. These two experimental datasets cover different pressure ranges, release orientations

(vertical and horizontal), and measurement methods, providing robust dual evidence for the model's generalizability.

2.5.1. Validation for Ultra-High-Pressure Vertical Jet Flames

To validate the predictive accuracy of the model under the most severe leakage scenario for onboard high-pressure hydrogen storage systems, we selected the experimental data from the fire-induced emergency release tests of high-pressure hydrogen cylinders conducted by Zou et al. [33]. These experiments simulated the ultra-high-pressure transient release process where a temperature rise from heat exposure causes the activation of a thermally activated pressure relief device (TPRD) on a vehicle storage cylinder. With an extremely high initial pressure and a flow in a highly choked state, this scenario presents a critical test for the real-gas effect model. In the experiment, hydrogen was instantaneously released vertically upward from a cylinder at an initial pressure of 77.4 MPa through a sharp-edged circular orifice nozzle with a diameter $D = 2$ mm. A stable turbulent diffusion flame formed immediately after release. The flame morphology was recorded using high-speed photography, and the maximum flame length was reported.

Using the aforementioned experimental conditions as model inputs—$P_0 = 77.4$ MPa, $D = 2$ mm, $T_0 = 300$ K (assumed ambient temperature), discharge coefficient $C_d = 0.75$—the key step is determining the C_r^*. According to Table 1, $C_r^* = 0.632065$ at $P_0 = 70$ MPa and $T_0 = 300$ K. Using linear interpolation, the value of C_r^* at $P_0 = 77.4$ MPa and $T_0 = 300$ K is estimated to be approximately 0.625. Substituting this value into the integrated flame length model (Equation (8)) yields the calculated maximum safety flame length L_m. The following figure shows a photograph of the jet fire from this experiment. The maximum flame length measured in the experiment was 4.93 m, while the maximum safety flame length calculated by the numerical model (rounded to centimeters) was 6.10 m.

The physical meaning of L_m, as the maximum safe distance predicted by the model, lies in its purpose to define a safety boundary capable of encompassing all potential experimental observations, rather than simply aiming for precise alignment with a single experimental data point. In this case, the model prediction (6.10 m) is approximately 1.17 m higher than the maximum observed experimental value (4.93 m). This difference precisely reflects the reasonableness and necessity of the model as an engineering safety boundary. This discrepancy carries significant practical importance: conservative prediction is paramount in high-pressure hydrogen safety design. Actual leakage scenarios involve numerous uncertainties—such as environmental turbulence, humidity, obstacle-induced perturbations, and potential non-ideal release conditions—any of which could lead to a flame length exceeding the "typical" maximum measured in a controlled laboratory setting. By incorporating the real-gas effect correction and critical flow factor interpolation, the model provides a safety envelope value that covers potential extreme conditions. This 1.17 m margin constitutes critical safety redundancy designed to account for these very uncertainties. Therefore, the model's prediction being slightly higher than the experimental maximum is not a flaw, but rather an embodiment of its role as a safety-oriented tool, providing a conservative safety boundary for engineering applications, which holds significant positive implications for practical engineering. The figure below (Figure 3) shows the flame shape as recorded by the high-speed photography of this experiment.

To further highlight the enhancement in model accuracy achieved by introducing the C_r^*, this study conducted a comparative validation based on the same set of experimental data. In the research by Zou et al. [33], besides the flame length observations, the experimentally measured hydrogen mass flow rate was reported to be approximately $\dot{q}_m = 0.1$ kg/s. This value, representing the actual leakage rate obtained through direct or indirect experimental measurement, reflects the mass output under real flow conditions.

Using this as a benchmark, we calculated the mass flow rate for the same operating condition ($P_0 = 77.4$ MPa, $D = 2$ mm, $T_0 = 300$ K) using both the real-gas corrected model (Equation (7)) proposed in this study and the traditional ideal-gas model (Equation (4), with $C_i^* \approx 0.687$), applying a discharge coefficient of $C_d = 0.75$. The deviations of both predictions from the experimental value were then compared. The calculation results show that the ideal-gas model predicted a mass flow rate of $\dot{q}_{m,ideal} \approx 0.1126$ kg/s, resulting in a relative error of 12.6%. In contrast, the real-gas model incorporating $C_r^* \approx 0.625$ yielded a prediction of $\dot{q}_{m,real} \approx 0.1025$ kg/s, with a significantly reduced relative error of merely 2.5%.

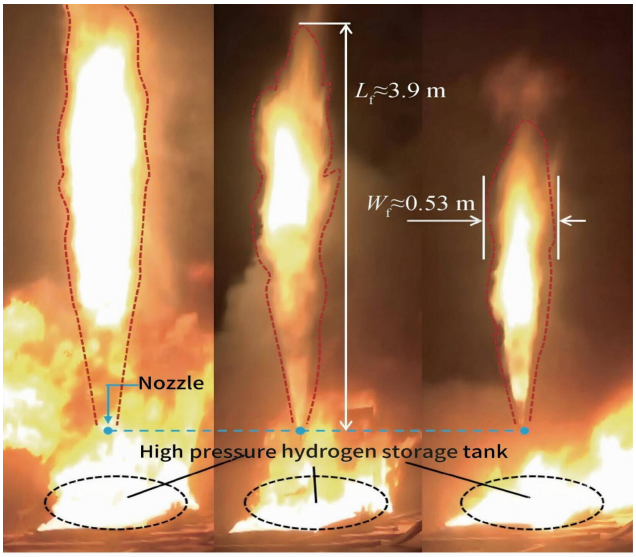


Figure 3. Experimental Jet Flame Length [33].

Regarding Table 2, this comparison clearly demonstrates that under ultra-high-pressure conditions, neglecting the real-gas effects of hydrogen leads to a systematic overestimation of the mass flow rate, which can subsequently cause significant deviations in flame length predictions. By dynamically correcting for C_r^*, the present model effectively captures the non-ideal flow behavior of high-pressure hydrogen. This enhancement fundamentally improves the accuracy in describing the physical leakage process at its source, thereby establishing a more solid theoretical foundation for the reliable prediction of flame length.

Table 2. Comparison of Model-Predicted Mass Flow Rates with Experimental Data.

Model/Data Category	Mass Flow Rate q_m (kg/s)	Relative Error Compared to the Experimental Value
Test measurement values (Zou et al. [33])	0.1	-
Predicted values of the ideal gas model ($C_i^* \approx 0.687$)	0.1126	12.60%
Predicted values of the real-gas model ($C_r^* \approx 0.625$)	0.1025	2.50%

2.5.2. Validation of Medium-to-High Pressure Horizontal Jet Flames

To further examine the model's robustness across a broader pressure range and validate its applicability for the common leakage direction of horizontal jets, we selected the systematic experimental data on horizontal jet flames from Zhang et al. [34]. This study

provides well-controlled steady-state leak conditions, making it suitable for validating the model in non-transient release scenarios. The experiment employed a horizontally aligned nozzle, where hydrogen was released from a high-pressure storage tank through a circular nozzle with a diameter $D = 2$ mm after pressure stabilization, forming a stable horizontal non-premixed jet flame.

Two typical steady-state pressure conditions were selected for validation:

Condition 1: $P_0 = 4$ MPa; Condition 2: $P_0 = 9$ MPa

The ambient pressure P_b was standard atmospheric pressure, satisfying the choked flow condition. Flame lengths were obtained via high-speed imaging combined with image processing methods. The fundamental model inputs were: $D = 0.002$ m, $T_0 = 300$ K, $C_d = 0.75$. For the 4 MPa condition, interpolation from Table 1 gives $C_r^* \approx 0.6858$; for the 9 MPa condition, $C_r^* \approx 0.6792$. These parameters were substituted into Equation (8) to calculate the respective maximum safety flame length L_m.

(1) For Condition 1 (4 MPa): The maximum flame length measured in the experiment was 1.81 m. The maximum safety flame length L_m calculated by the numerical model (rounded to centimeters) was 2.25 m, which is approximately 0.44 m higher than the maximum experimental observation.

(2) For Condition 2 (9 MPa): The maximum flame length measured in the experiment was 2.41 m. The maximum safety flame length L_m calculated by the numerical model (rounded to centimeters) was 2.97 m, which is approximately 0.56 m higher than the maximum experimental observation. The Table 3 below can facilitate the comparison and analysis of the data.

Table 3. Comparison of predicted and measured flame lengths under different leakage scenarios.

Verification Project	Experimental Conditions	Experimental Measurement Values	Model Prediction Value	Safety Margin
Verification of Ultra-High Pressure Vertical Jet Flame	Initial pressure: P_0 = 77.4 MPa Nozzle diameter: D = 2 mm Initial temperature: T_0 = 300 K (Assuming the ambient temperature) Flow coefficient: C_d = 0.75 Critical flow factor of real gases: $C_r^* \approx 0.625$ Discharge direction: vertically upward	4.93 m	6.10 m	1.17 m
Verification of medium and high-pressure level jet flames	Condition 1: Initial pressure: P_0 = 4 MPa Nozzle diameter: D = 2 mm Initial temperature: T_0 = 300 K (Assuming the ambient temperature) Flow coefficient: C_d = 0.75 Critical flow factor of real gases: $C_r^* \approx 0.6858$ Discharge direction: Horizontal	1.81 m	2.25 m	0.44 m
	Condition 2: Initial pressure: P_0 = 9 MPa Nozzle diameter: D = 2 mm Initial temperature: T_0 = 300 K (Assuming the ambient temperature) Flow coefficient: C_d = 0.75 Critical flow factor of real gases: $C_r^* \approx 0.6792$ Discharge direction: Horizontal	2.41 m	2.97 m	0.56 m

2.6. Error Analysis

The discrepancies observed in the results of this study can be primarily attributed to the inherent limitations at four levels: flame turbulence fluctuations, the measurement system, and the theoretical model itself.

At the level of flame turbulence fluctuations, hydrogen jet flames are high-Reynolds-number turbulent diffusion flames whose instantaneous morphology is governed by turbulent eddies, resulting in continuous fluctuations and significant temporal variability in flame length. Furthermore, the turbulent structure enhances air entrainment and alters the local mixing rate, thereby affecting flame stretching and lift-off, which introduces additional random errors into length measurements.

At the measurement level, the acquisition of key parameters such as flame length, pressure, and flow velocity relies on sensor accuracy and response characteristics. Even with high-precision instrumentation, systematic errors, including calibration offsets and non-linearity errors, can introduce measurement uncertainties on the order of 0.5% to 1%. Concurrently, environmental disturbances during experiments, such as subtle variations in temperature, humidity, and air currents, can interfere with flame morphology and gas flow fields. Hydrogen's exceptionally high diffusion coefficient renders it particularly sensitive to such perturbations.

At the theoretical model level, despite the incorporation of real-gas effects, the model remains grounded in idealized assumptions such as steady-state flow, complete combustion, and an isothermal process. It does not fully account for potential temperature variations due to the Joule-Thomson effect that may occur in actual leakage scenarios.

3. Discussion and Analysis

Based on the validated flame length model (Equation (8)) and the real-gas mass flow rate model (Equation (7)), this section systematically analyzes the quantitative influence of two key parameters—storage pressure P_0 and D—on both flame length and mass flow rate.

3.1. Quantitative Relationship Between Flame Length and Key Parameters

The analysis considers the following parameter ranges: $P_0 \in [10,\ 100]$ MPa and $D \in [0.1,\ 3]$ mm, with the temperature held constant at $T_0 = 300$ K. The mathematical model, obtained by implementing the relevant equations in MATLAB R2025a, is presented in the figure below (red curve: maximum safety flame length; blue curve: optimal-fit flame length).

Through parametric analysis of the established model, the variation patterns of flame length with storage pressure (P_0) and leakage orifice diameter (D) are quantitatively presented. The three-dimensional surface plot (Figure 4) clearly shows that both the optimal-fit flame length (L_{FL}), representing typical conditions, and the maximum safety flame length (L_{FM}), serving as the basis for safety thresholds, increase significantly with rising P_0 and D, exhibiting a distinct nonlinear growth trend. The scaling relationship derived from the theoretical model is as follows:

$$L \propto \left(D^3 \cdot P_0\right)^{0.347}$$

The analysis reveals that the exponent for the orifice diameter D is approximately 1.041, while that for the pressure P_0 is about 0.347. This indicates that a slight increase in orifice diameter has a far greater driving effect on flame length than a proportional increase in pressure. Specifically, the flame lengthening caused by doubling the orifice diameter would require a several-fold increase in pressure to achieve an equivalent effect. This quantitative conclusion underscores the critical importance of controlling leakage orifice size in inherent safety design.

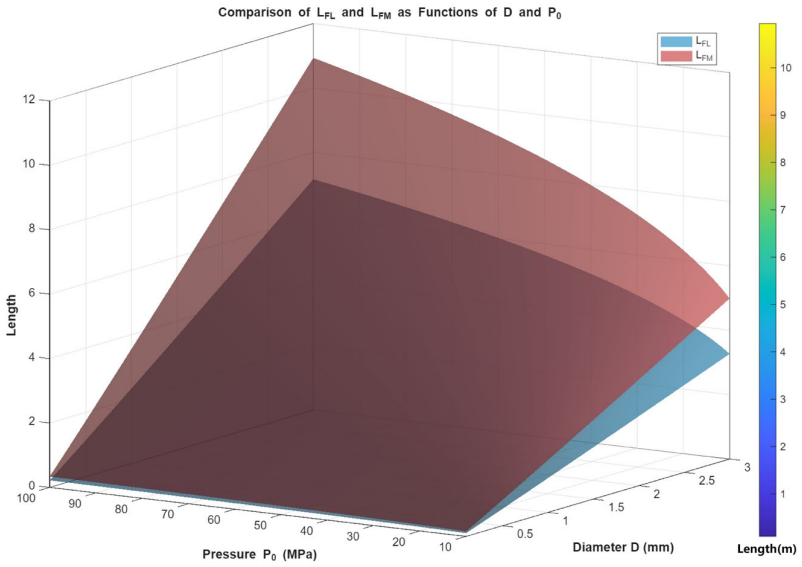


Figure 4. Three-dimensional response surface of flame length L (m) as a function of storage pressure P_0 (MPa) and leakage orifice diameter D (mm) at constant temperature T_0 = 300 K.

In summary, the model and its visual outputs translate abstract theoretical equations into specific predictions of the flame scale for different accident scenarios (varying pressure levels and leakage sizes).

Figure 5 above presents a contour plot of the optimal-fit flame length (L_{FL}) and the maximum safety flame length (L_{FM}) as functions of the initial pressure (P_0) and the release orifice diameter (D).

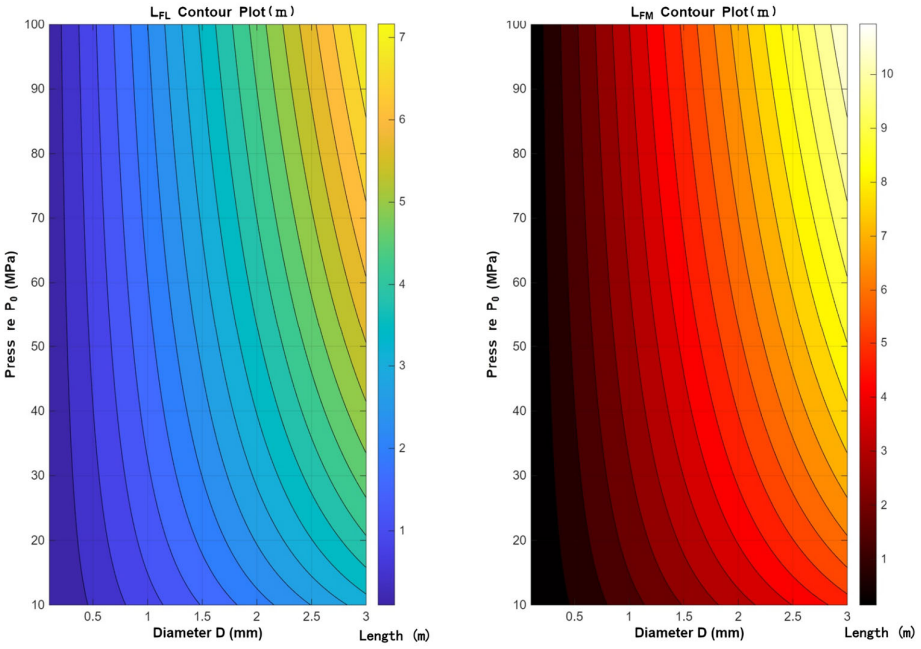


Figure 5. Contour Plot of Optimal-Fit and Maximum Safety Flame Lengths versus Orifice Diameter and Initial Storage Pressure.

3.2. Parameter Sensitivity Analysis and Identification of Dominant Factors

By comparing Figures 6 and 7, it can be observed that under the same degree of variation, the influence of the aperture on the flame length is much greater than that of the pressure. The parameter sensitivity analysis clearly reveals the magnitude difference in the influence of aperture and pressure on the flame length. Under the same degree of variation,

the influence of the aperture is dominant. For instance, when the aperture increases from 1 mm to 3 mm, the flame length increases by approximately three times; while when the pressure rises from 20 MPa to 100 MPa, the increase in the flame length is relatively limited, only about 1.5 to 2 times. Therefore, from the perspective of controlling the risk of fire consequences, optimizing the design of hardware components such as valves and flanges to reduce the potential leakage size is more effective in mitigating the accident consequences compared to simply limiting the system's working pressure.

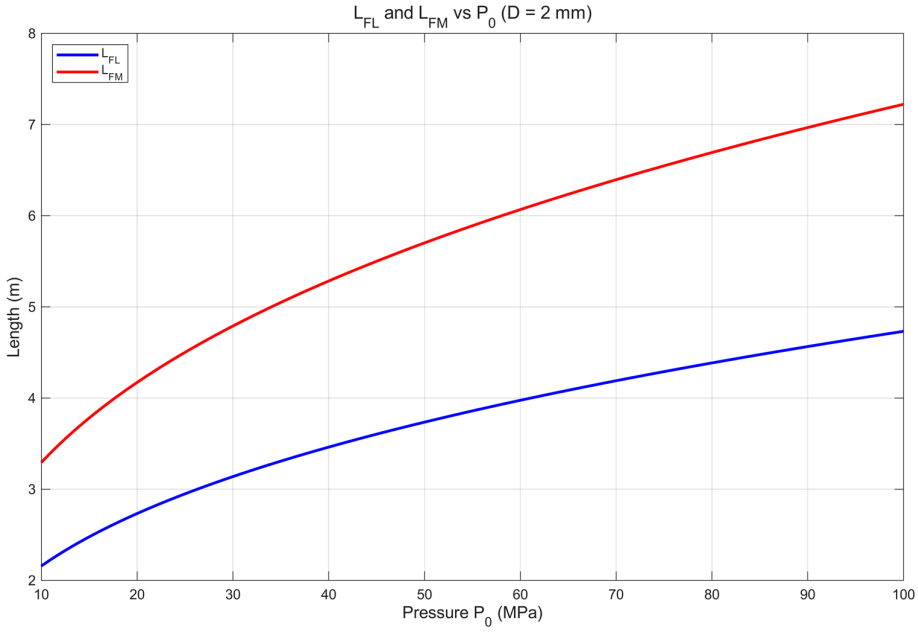


Figure 6. Variation of Optimal-Fit (L_{FL}) and Maximum Safety (L_{FM}) Flame Lengths with Initial Pressure (P_0) for a Leakage Orifice Diameter of D = 2 mm.

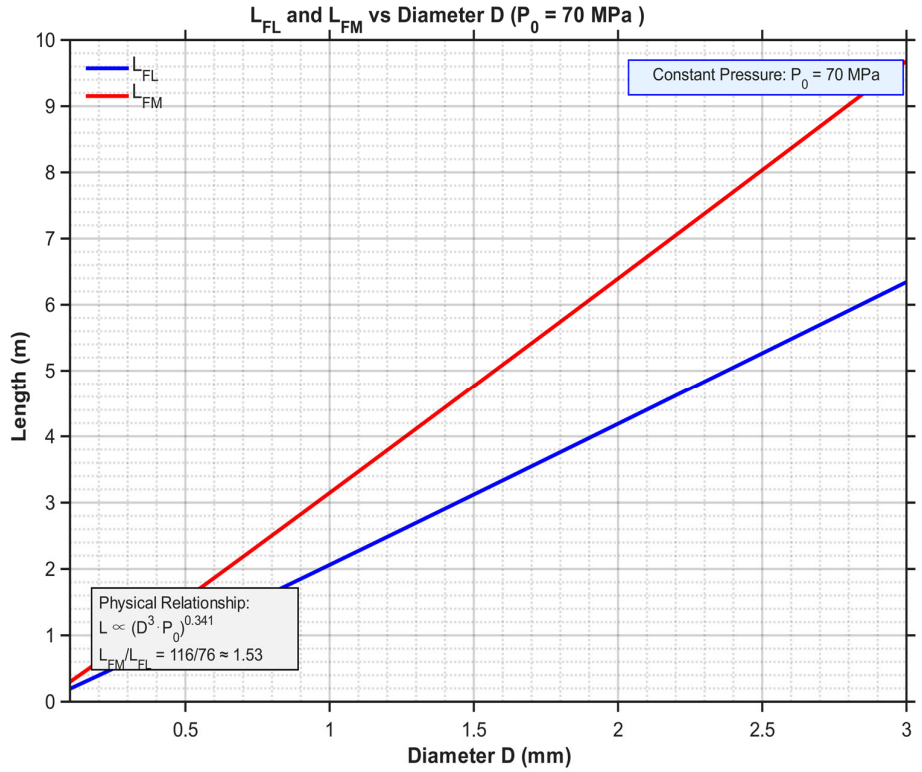


Figure 7. Variation of Optimal-Fit (L_{FL}) and Maximum Safety (L_{FM}) Flame Lengths with Orifice Diameter (D) for an Initial Pressure of P_0 = 70 MPa.

3.3. Evolution and Implications of Leakage Mass Flow Rate

This work systematically investigates the influence of initial pressure (P_0) and nozzle diameter (D) on the jet dynamics of hydrogen, focusing on flame length and velocity evolution during high-pressure hydrogen releases through theoretical modeling and experimental validation. The relationship between mass flow rate and P_0/D, as shown in Figure 8, elucidates the flow characteristics of hydrogen jets across a broad parameter range, providing a critical foundation for flame behavior prediction and safety assessment.

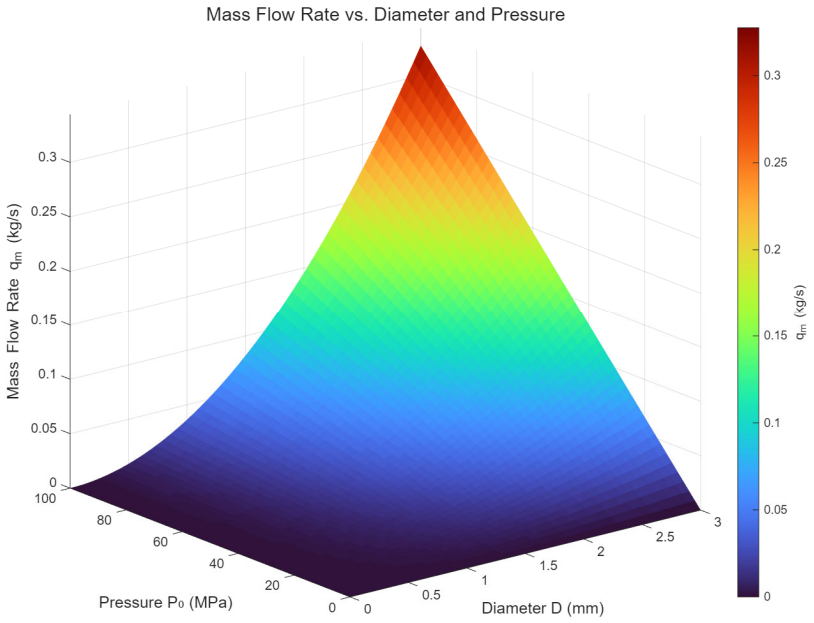


Figure 8. Variation of the Mass Flow Rate q_m with Storage Pressure P_0 and Leakage Orifice Diameter D for High-Pressure Hydrogen.

The most direct conclusion from Figures 9 and 10 is that under the high-pressure condition of 70 MPa, the leakage mass flow rate (and by extension, the mass flow rate itself) is proportional to the square of the orifice diameter.

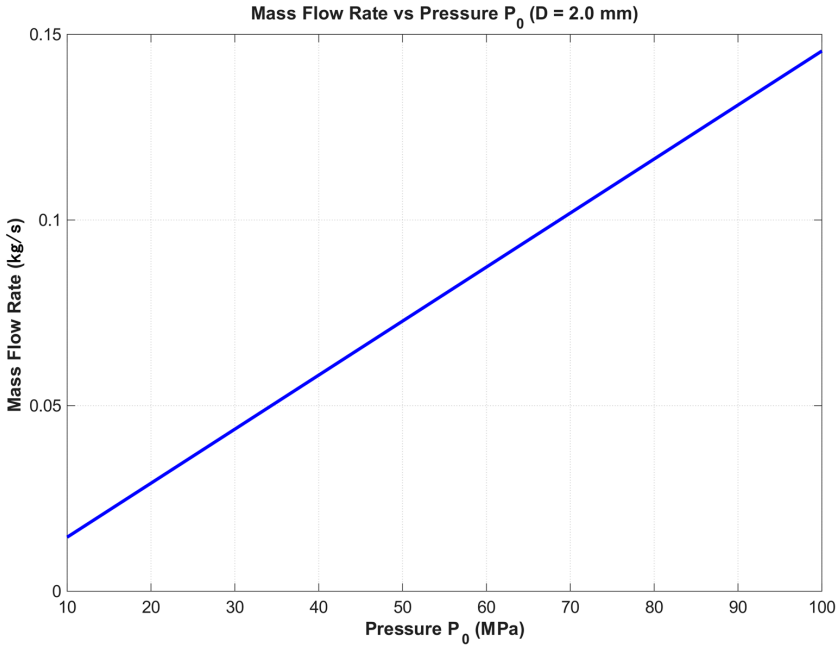


Figure 9. Plot of Real-Gas Mass Flow Rate versus Storage Pressure at a Fixed Leakage Orifice Diameter (D = 2 mm).

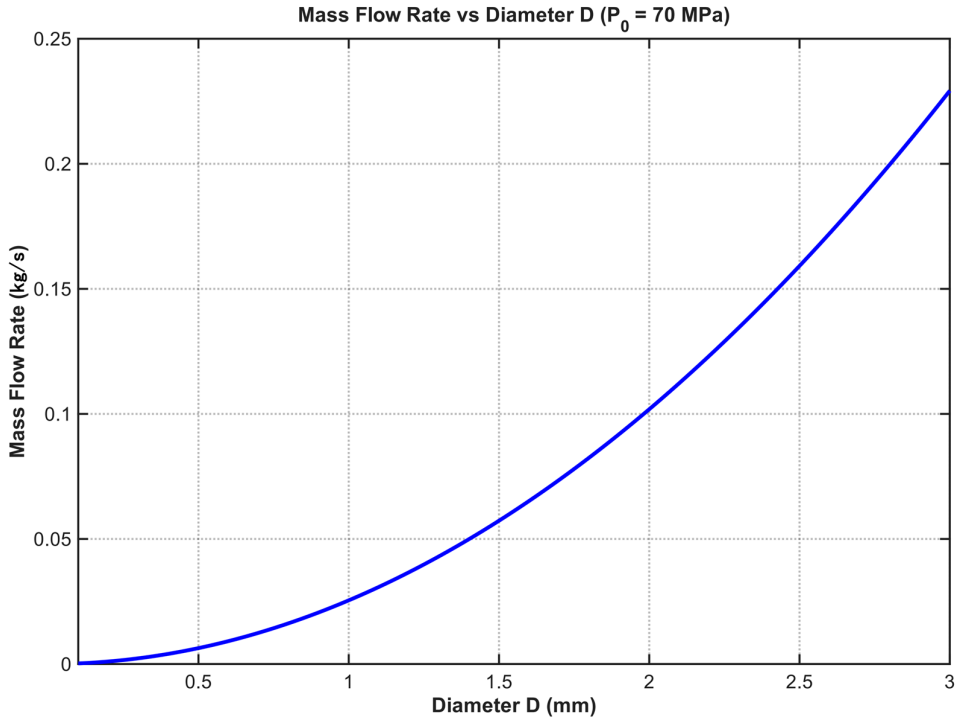


Figure 10. Plot of Real-Gas Mass Flow Rate versus Leakage Orifice Diameter at a Fixed Storage Pressure (P_0 = 70 MPa).

The figure demonstrates that as the diameter increases from 0.5 mm to 3 mm—a mere fivefold increase—the mass flow rate, governed by the quadratic relationship, surges by approximately 35 times. This implies that under identical high pressure, the hydrogen leak rate and consequent energy release rate from a 3 mm orifice are far from comparable to those from a minor crack (e.g., 0.5 mm). This conclusion is of paramount importance for hydrogen safety engineering: in high-pressure systems, even very minor structural damage can lead to catastrophic leakage consequences. When designing safety measures, such as explosion-proof separation distances and ventilation requirements, this nonlinear scaling effect must be fully accounted for.

Flame length is closely related to the fuel mass flow rate, typically following a power-law relationship. Therefore, the pattern of mass flow rate variation with diameter revealed in this figure directly dictates the corresponding trend of flame length with diameter. It can be unequivocally stated that since the mass flow rate increases with D^2, the flame length is expected to increase approximately linearly with D (or a power of D). This establishes a clear logical bridge for the subsequent parametric investigation.

Verification of the Square-*D*'s Law and Its Engineering Significance

In the blocked flow state, by using Formula (7) and the leakage area $A_t = \frac{\pi D^2}{4}$, it can be derived that the basic proportional relationship between the mass flow rate and the leakage aperture as well as the pressure is as follows:

$$q_{m,real} \propto D^2 \cdot P_0$$

This relationship demonstrates that mass flow rate is proportional to the square of the leakage aperture—a principle known as "Square-*D*'s Law." This law explains the nonlinear surface shown in Figure 8. At small apertures (D), the D^2 term diminishes the visible influence of P_0 on mass flow rate ($\dot{m}$). As D increases, however, the squaring effect amplifies $\dot{m}$, making it highly sensitive to changes in P_0.

Figure 10 presents the variation in real-gas mass flow rate ($\dot{m}$) with leakage orifice diameter (D) at a fixed storage pressure of P_0 = 70 MPa (T_0 = 300 K), which illustrates the quadratic relationship (Square-D's Law) within the studied diameter range of 0.5–3 mm under choked flow conditions. In addition, for the specific ultra-high-pressure leakage scenario (77.4 MPa, D = 2 mm) shown in Table 2, the real-gas corrected model yields a mass flow rate prediction with a relative error of merely 2.5%. This high precision in predicting the mass flow rate for this representative ultra-high-pressure case forms a solid foundation for the reliability of the subsequent flame-length predictions, given the strong correlation between fuel mass flow rate and jet fire length.

"The Square-D's Law" has clear guiding significance for engineering safety:

Risk control priority: Compared to controlling the storage pressure, limiting the potential leakage aperture is a more effective risk mitigation strategy. A slight increase in the aperture size will result in a significant expansion of the mass flow rate and the range of flame hazards.

Safety design basis: This law provides quantitative design constraints for the release ports of key components such as pressure relief devices and connectors, as well as the allowable defect sizes. The goal should be to minimize the "credible maximum leakage diameter".

Foundation of consequence assessment: In risk assessment and emergency response plans, great attention must be paid to "large-diameter" leakage scenarios, as their consequences exhibit non-linear growth.

4. Conclusions

Through the development and validation of a refined jet flame length prediction model applicable to high-pressure hydrogen leakage, this study leads to the following conclusions:

(1) The key innovation of this study lies in the introduction of a pressure- and temperature-dependent C_r^*, which effectively corrects the mass flow rate calculation error arising from hydrogen's deviation from the ideal-gas assumption under high-pressure conditions. The model demonstrates strong predictive performance in two representative scenarios: ultra-high-pressure (77.4 MPa) vertical jets and medium-to-high-pressure (4–9 MPa) horizontal jets, meeting the accuracy requirements for engineering applications and thereby validating its accuracy and reliability.

(2) Through systematic parametric analysis, a quantitative scaling relationship between flame length (L), storage pressure (P_0), and D was established as $L \propto D^{1.041} \cdot P_0^{0.347}$. This relationship reveals that the leakage orifice diameter is the dominant factor governing flame length, exerting an influence approximately three times greater than that of the storage pressure.

This study transforms the theoretical model into intuitive parameter influence maps that can be applied in engineering practice. The model results provide a basis for safety distance demarcation, leak monitoring threshold setting, and inherent safety design in scenarios such as hydrogen refueling stations, storage depots, and onboard systems.

5. Future Expectations

Future research directions include: (1) advancing beyond the current model's idealized assumption of a static, wind-free environment by incorporating common real-world factors such as ambient winds and spatial obstructions to enhance its applicability under truly complex conditions; (2) conducting further experimental studies, particularly under a broader range of conditions involving higher pressures, larger orifice diameters, and varied leak orientations, to enable comprehensive validation and calibration of the model's predictive performance under coupled multi-factor effects; (3) the current model adopts

a simplified assumption of standard dry air (21% O_2/79% N_2) to focus on the macro-scale problems dominated by the leakage fluid dynamics. Future research could explore using environmental humidity as a variable to assess its potential impact under specific extreme conditions.

Author Contributions: Conceptualization, J.-Q.L. and J.-T.K.; methodology, J.-Q.L. and Y.W.; software, J.-W.L., X.-L.L. and Y.F.; validation, J.-W.L., X.-L.L. and Y.F.; formal analysis, R.-Q.S., E.-M.Z., Y.-M.D. and Y.F.; investigation, R.-Q.S., J.-W.L., X.-L.L. and E.-M.Z.; resources, J.-Q.L., Y.W. and J.-T.K.; data curation, J.-W.L., X.-L.L. and Y.F.; writing—original draft preparation, Y.-M.D., J.-W.L., X.-L.L. and Y.F.; writing—review and editing, Y.-M.D., Y.W., J.-Q.L. and J.-T.K.; visualization, R.-Q.S., E.-M.Z.; supervision, J.-W.L. and X.-L.L.; project administration, J.-Q.L. and Y.W.; funding acquisition, J.-Q.L. All authors have read and agreed to the published version of the manuscript.

Funding: This study was supported by the result of receiving the support for the Fundamental Research Funds for the Central Universities (JD2527) and the National Natural Science Foundation of China (Grant No. 52505242).

Data Availability Statement: Data are contained within the article.

Acknowledgments: This research is also the result of receiving the support for the 2025 college student's innovation and entrepreneurship training program project, China.

Conflicts of Interest: The authors declare no conflicts of interest.

References

1. Sadeq, A.M.; Homod, R.Z.; Hussein, A.K.; Togun, H.; Mahmoodi, A.; Isleem, H.F.; Patil, A.R.; Moghaddam, A.H. Hydrogen energy systems: Technologies, trends, and future prospects. *Sci. Total Environ.* **2024**, *939*, 173622. [CrossRef]
2. Kourougianni, F.; Arsalis, A.; Olympios, A.V.; Yiasoumas, G.; Konstantinou, C.; Papanastasiou, P.; Georghiou, G.E. A comprehensive review of green hydrogen energy systems. *Renew. Energy* **2024**, *231*, 120911. [CrossRef]
3. Halder, P.; Babaie, M.; Salek, F.; Shah, K.; Stevanovic, S.; Bodisco, T.A.; Zare, A. Performance, emissions and economic analyses of hydrogen fuel cell vehicles. *Renew. Sustain. Energy Rev.* **2024**, *199*, 114543. [CrossRef]
4. Yang, N.; Deng, J.; Wang, C.; Bai, Z.; Qu, J. High pressure hydrogen leakage diffusion: Research progress. *Int. J. Hydrogen Energy* **2024**, *50*, 1029–1046. [CrossRef]
5. Zou, Q.; Tian, Y.; Han, F. Prediction of state property during hydrogen leaks from high-pressure hydrogen storage systems. *Int. J. Hydrogen Energy* **2019**, *44*, 22394–22404. [CrossRef]
6. Cui, G.; Li, Y.; Wu, D.; Li, H.; Liu, H.; Xing, X.; Liu, J. The Progress of Autoignition of High-Pressure Hydrogen Gas Leakage: A Comprehensive Review. *Fire* **2024**, *7*, 268. [CrossRef]
7. Liu, X.Y.; Sun, Z.Y.; Yi, Y. Progress in spontaneous ignition of hydrogen during high-pressure leakage with the considerations of pipeline storage and delivery. *Appl. Energy Combust. Sci.* **2024**, *20*, 100290. [CrossRef]
8. Lin, W.; Wang, Z.; Wang, G.; Jiang, J.; Wu, J.; Ni, L.; Zhou, R.; Zhang, M.; Ma, L. Numerical Investigation of Spontaneous Ignition During Pressurized Hydrogen Release: Effects of Burst Disk Shape and Opening Characteristics. *Fire* **2025**, *8*, 246. [CrossRef]
9. Zhou, S.; Xiao, J.; Luo, Z.; Kuznetsov, M.; Chen, Z.; Jordan, T.; Banuti, D.T. Analysis of spontaneous ignition of hydrogen-enriched methane in a rectangular tube. *Proc. Combust. Inst.* **2024**, *40*, 105681. [CrossRef]
10. Pan, X.; Lu, L.; Zhang, T.; Jiang, Y.; Li, Y.; Wang, Z.; Hua, M.; Jiang, J. Effect of the leak port area and tube length on suppression of spontaneous ignition of high-pressure hydrogen. *J. Energy Storage* **2023**, *74*, 109396. [CrossRef]
11. Huang, Q.; Sun, Z.Y.; Du, Y.L.; Li, J.Y. Dynamic process of hydrogen flow and spontaneous combustion in tubes featuring different configurations after leakage from 35 and 70 MPa. *Green Energy Resour.* **2025**, *3*, 100127. [CrossRef]
12. Ayi, C.K.; Sripaul, E.; Vaddiraju, S.; Khan, F. How is hydrogen autoignition an extrinsic property? *Int. J. Hydrogen Energy* **2026**, *197*, 152612. [CrossRef]
13. Cui, G.; Li, Y.; Zhang, Q.; Yin, J.; Wu, D.; Xing, X.; Liu, J. Study on characterization of flame propagation of spontaneous ignition caused by high-pressure hydrogen leakage. *Case Stud. Therm. Eng.* **2024**, *64*, 105415. [CrossRef]
14. Bradley, D.; Gaskell, P.H.; Gu, X.; Palacios, A. Jet flame heights, lift-off distances, and mean flame surface density for extensive ranges of fuels and flow rates. *Combust. Flame* **2016**, *164*, 400–409. [CrossRef]
15. Al-Tayyar, M.A.; AlKhafaji, D.; Shahad, H.A. A Review on Flame Height and Structure and Pollutants Formation. *Neuro Quantology* **2022**, *20*, 2946–2968.

16. Lv, J.; Wang, Q.; Tang, F.; Sun, X. The evolution of flame geometrical characteristics and air entrainment of inclined jet flames. *Process Saf. Environ. Prot.* **2023**, *178*, 414–422. [CrossRef]
17. Ab Aziz, N.S.; Kasmani, R.M. Projected flame length and flame extension length of horizontal buoyant jet flames. *J. Phys. Conf. Ser.* **2022**, *2259*, 012027. [CrossRef]
18. Wang, Q.; Lu, A.; Chang, L.; Wang, B. A new mathematical method for quantifying flame trajectory length of inclined buoyant jet fires in crosswind. *J. Therm. Anal. Calorim.* **2022**, *147*, 11363–11371. [CrossRef]
19. Shen, J.; Zou, X.; Zhang, A.; Zhang, K.; Gao, W. Study on high-pressure hydrogen leakage characteristics under different shapes of nozzles. *Int. J. Hydrogen Energy* **2024**, *73*, 619–631. [CrossRef]
20. Cerbarano, D.; Tieghi, L.; Delibra, G.; Lo Schiavo, E.; Minotti, S.; Corsini, A. Characterization of High-Pressure Hydrogen Leakages. *J. Eng. Gas Turbines Power* **2024**, *146*, 051019. [CrossRef]
21. Gain, B.; Daniel, S.; Bilal, M.; Yousuf, M.; Tian, Z. Experimental Studies of RP-3 Partially Premixed Jet Flames. *J. Therm. Sci.* **2025**, *34*, 780–788. [CrossRef]
22. Gao, Y.; Dou, Y.; Tao, C.; He, P.; Zhang, X.; Huang, X.; Zhou, X. Numerical analysis on combustion characteristics of diffusion jet flame under different gravity environments. *Case Stud. Therm. Eng.* **2023**, *50*, 103481. [CrossRef]
23. Sun, B.; Loughnan, T. Consequence analysis of vapour cloud explosion from the release of high-pressure hydrogen storage. *Int. J. Hydrogen Energy* **2024**, *80*, 1137–1150. [CrossRef]
24. Liu, H.; Wang, W.; Song, H.; Kuang, T.; Li, Y.; Guang, Y. Consequence Analysis of Liquid Hydrogen Leakage from Storage Tanks at Urban Hydrogen Refueling Stations: A Case Study. *Hydrogen* **2025**, *6*, 58. [CrossRef]
25. Zhang, Z.; Shang, M. Research on hydrogen leakage and diffusion mechanism in hydrogenation station. *Sci. Rep.* **2024**, *14*, 3363. [CrossRef]
26. Wang, Y.; Xu, C.; Zhao, G.; Zeng, Y.; Han, R.; He, T. Numerical simulation study on hydrogen leakage and explosion of hydrogen fuel cell buses. *Sci. Rep.* **2025**, *15*, 31976. [CrossRef]
27. Li, B.; Han, B.; Li, Q.; Gao, W.; Guo, C.; Lv, H.; Liu, Y.; Jin, X.; Bi, M. Study on hazards from high-pressure on-board type III hydrogen tank in fire scenario: Consequences and response behaviours. *Int. J. Hydrogen Energy* **2022**, *47*, 2759–2770. [CrossRef]
28. Weng, Z.; Tan, Y.; Maxwell, B.M.; Mével, R. Real gas effects on the dynamics of a reactive diffusion layer: Application to the study of spontaneous ignition limit of pressurized hydrogen jet. *Proc. Combust. Inst.* **2024**, *40*, 105370. [CrossRef]
29. Nabizadeh, A.; Jamiolahmady, M. A methodology for predicting choked compressible gas flow in pores using dimensional analysis. *Phys. Fluids* **2025**, *37*, 096124. [CrossRef]
30. HyResponder Consortium. Hazard distances from hydrogen flames and fire fighting (Lecture 9). In *European Train the Trainer Programme for Responders*; Fuel Cells and Hydrogen Joint Undertaking (FCH JU): Brussels, Belgium, 2021.
31. Bobovnik, G.; Mickan, B.; Sambol, P.; Maury, R.; Kutin, J. Investigation of the discharge coefficient in the laminar boundary layer regime of critical flow Venturi nozzles calibrated with different gases including hydrogen. *Measurement* **2023**, *217*, 113134. [CrossRef]
32. Ding, H.; Wang, C.; Zhao, Y. Flow characteristics of hydrogen gas through a critical nozzle. *Int. J. Hydrogen Energy* **2014**, *39*, 3947–3955. [CrossRef]
33. Zou, L.; Li, B.; Han, B.; Liu, Y.; Song, C.; Jin, X. Risk prediction of thermal radiation from jet fire of onboard hydrogen storage tanks. *J. Tsinghua Univ. (Sci. Technol.)* **2025**, *65*, 2149–2156.
34. Zhang, A.; Zou, X.; Shen, J.; Li, Y.; Gao, W. Experimental investigation on hydrogen jet flame behavior and temperature distribution with different shapes of outlet. *Int. J. Hydrogen Energy* **2024**, *63*, 844–856. [CrossRef]

Disclaimer/Publisher's Note: The statements, opinions and data contained in all publications are solely those of the individual author(s) and contributor(s) and not of MDPI and/or the editor(s). MDPI and/or the editor(s) disclaim responsibility for any injury to people or property resulting from any ideas, methods, instructions or products referred to in the content.